Received: 1 December 2017 | Revised: 22 August 2018 | Accepted: 8 October 2018

DOI: 10.4218/etrij.2017-0266

ORIGINAL ARTICLE

WILEY ETRI Journal

Low-complexity de-mapping algorithms for 64-APSK signals

Junwei Bao[1,2,3] | **Dazhuan Xu**[1,2] | **Xiaofei Zhang**[1,2] | **Hao Luo**[1,2]

[1]College of Electronic and Information Engineering, Nanjing University of Aeronautics and Astronautics, Nanjing, China

[2]Jiangsu Key Laboratory of Internet of Things and Control Technologies, Nanjing University of Aeronautics and Astronautics, Nanjing, China

[3]College of Science, Nanjing University of Aeronautics and Astronautics, Nanjing, China

Correspondence
Dazhuan Xu, College of Electronic and Information Engineering, Nanjing University of Aeronautics and Astronautics, Nanjing, China.
Email: xudazhuan@nuaa.edu.cn

Funding Information
This research was supported by the National Natural Science Foundation of China (grant nos 61371169 and 61471192).

Due to its high spectrum efficiency, 64-amplitude phase-shift keying (64-APSK) is one of the primary technologies used in deep space communications and digital video broadcasting through satellite-second generation. However, 64-APSK suffers from considerable computational complexity because of the de-mapping method that it employs. In this study, a low-complexity de-mapping method for (4 + 12 + 20 + 28) 64-APSK is proposed in which we take full advantage of the symmetric characteristics of each symbol mapping. Moreover, we map the detected symbol to the first quadrant and then divide the region in this first quadrant into several partitions to simplify the formula. Theoretical analysis shows that the proposed method requires no operation of exponents and logarithms and involves only multiplication, addition, subtraction, and judgment. Simulation results validate that the time consumption is dramatically decreased with limited degradation of bit error rate performance.

KEYWORDS
64-APSK, de-mapping, DVB-S2, log likelihood ratio, log-MAP, low complexity, max-log approximation (Max-Log-MAP)

1 | INTRODUCTION

With the increasing demands for high data rates with real-time communication systems, high-order modulation-demodulation techniques such as multiple amplitude-shift keying (M-APSK), in which each mapped symbol consists of several bits, is utilized to promote spectrum utilization efficiency. M-APSK is a combined modulation system of ASK and phase-shift keying (PSK) that uses different numbers of constellation points uniformly located on concentric rings. This system can effectively reduce peak-to-average power ratio (PAPR) and remain robust to nonlinear channels. M-APSK is widely applied to satellite broadcasting and space communications to increase transmission capacity because of the regularity of the constellation and the simple implementation of modulation or demodulation [1]. According to 131.2-B-1 from the Consultative Committee for Space Data Systems (CCSDS), M-APSK is the principal model for space data systems [2]. It is also one of the main technologies of DVB-S2, which was devised for digital satellite broadcasting by the European Telecommunications Standards Institute (ETSI) [3].

However, an M-APSK constellation is neither a single circular nor rectangular type like the PSK and QAM constellations, respectively. The inherent high computational complexity of demodulation hinders M-APSK from practical applications. Once the channel codes, such as low-density parity check (LDPC) or Turbo codes, are adopted, the decoders usually request the log likelihood ratio (LLR) from the demodulators for every bit, where the computational complexity increases exponentially with the modulation order of the system. Moreover, the computational complexity of the max-log-MAP is proportional to the constellation size, which makes it is unsuitable for large constellations.

In recent years, considerable effort has been devoted to devising low-complexity de-mapping methods. In [4–6], symmetric characteristics are exploited to reduce the number of calculations by decreasing possible constellation points during the LLR calculation of 16-APSK. In [7–9], the original constellation of 32-APSK is modified by relocating the symbols to reduce the computational complexity. In [10], an APSK constellation based on the kite structure is proposed that outperforms the corresponding PSK. Linear region for each bit in an APSK constellation is introduced in [11], where the coefficients are computed beforehand and stored in a look-up table. LLR can then be achieved through a binary search using the look-up table. The complexity of this method grows linearly with the number of bits rather than exponentially with the number of constellation points. The methods in [12–14] investigate the problem of reducing the complexity for (16 × 4)64-APSK and (32 × 8)256-APSK. In addition, a simplified method [15–17] for LLR in 32-APSK is proposed to reduce the computational complexity considerably.

In this study, we propose a simplified de-mapping method in which the symmetric characteristics of each symbol mapping of a (4 + 12 + 20 + 28)64-APSK constellation are fully utilized, and simplified calculation formulas are derived. The proposed method involves only a few calculations of addition, subtraction, and multiplication with no look-up table. This greatly reduces the computational complexity and time consumption as compared with the traditional log-MAP and max-log-MAP de-mapping algorithms. BER simulations over AWGN and Rayleigh fading channels verify the effectiveness and superiority of the proposed de-mapping method.

The remainder of this paper is organized as follows. The constellation of 64-APSK and traditional de-mapping algorithms are introduced in Section 2. The derivation of the simplified de-mapping method is described in Section 3. In Section 4, calculations are analyzed. Simulation results are provided in Section 5 and a conclusion is given in Section 6.

2 | 64-APSK CONSTELLATION AND TRADITIONAL SOFT DE-MAPPING

2.1 | Constellation of 64-APSK

(4 + 12 + 20 + 28)64-APSK is a combined modulation system of ASK and PSK, in which the modulation constellation is composed of four concentric rings, as shown in Figure 1.

$$S = \begin{cases} R_1 \exp\left[j \times \left(\frac{2\pi}{n_1} i_1 + \varphi_1\right)\right], & i_1 = 1, \cdots, n_1 \\ R_2 \exp\left[j \times \left(\frac{2\pi}{n_2} i_2 + \varphi_2\right)\right], & i_2 = 1, \cdots, n_2 \\ R_3 \exp\left[j \times \left(\frac{2\pi}{n_3} i_3 + \varphi_3\right)\right], & i_3 = 1, \cdots, n_3 \\ R_4 \exp\left[j \times \left(\frac{2\pi}{n_4} i_4 + \varphi_4\right)\right], & i_4 = 1, \cdots, n_4 \end{cases} \quad (1)$$

where R_k, n_k, i_k, and φ_k denote the radius, number of points, order of constellation points, and phase shift of the kth ring, respectively, and n_k is 4, 12, 20, and 28, when $k = 1, 2, 3$, and 4, respectively.

When a mapped symbol is transmitted over an AWGN channel, the output of the receiver can be represented by:

$$r = A \times S + N, \quad (2)$$

where A denotes the channel gain matrix and N is the additive white Gaussian noise matrix with variance σ^2.

$$r = I_r + j \times Q_r = \rho_r \times \exp(j \times \theta_r), \quad (3)$$

where I_r and Q_r are real and imaginary parts of received signal r,

$$\rho_r = \sqrt{I_r^2 + Q_r^2}, \quad (4)$$

$$\theta_r = \tan^{-1}\left(\frac{Q_r}{I_r}\right). \quad (5)$$

2.2 | Traditional soft de-mapping

To fully utilize the information contained in the received signal with channel coding, soft de-mapping methods are proposed such as log-MAP and max-log-MAP.

Typically, a transmitted symbol S is represented by six bits, b_5, b_4, b_3, b_2, b_1, and b_0 in the order from most significant bit (MSB) to least significant bit (LSB). This means

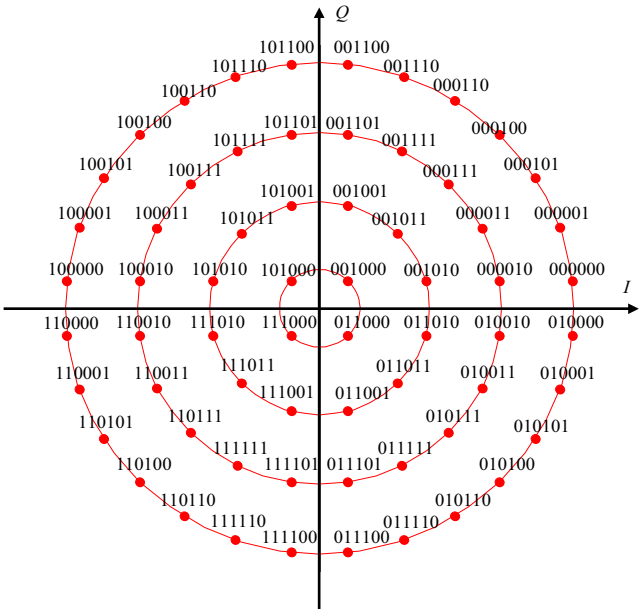

FIGURE 1 Constellation diagram and bits-to-symbol mapping of 64-APSK

$b_i(s)$ is the ith bit of the symbol and its soft output from the receiver is presented by:

$$\Lambda_i(r) = \ln\left(\frac{p(r|b_i(s)=0)}{p(r|b_i(s)=1)}\right), \tag{6}$$

where $b_i(s)$ can take only the value of 0 and 1. We define $S_i^{(0)}$ and $S_i^{(1)}$ as:

$$\begin{aligned} S_i^{(0)} &= \{s|b_i(s)=0, s\in S\}, \\ S_i^{(1)} &= \{s|b_i(s)=1, s\in S\}. \end{aligned} \tag{7}$$

Assume that all bits are transmitted with the same probability over the AWGN channel [18]:

$$\begin{aligned} \Lambda_i(r) &= \ln\left(\frac{\sum_{s\in S_i^{(0)}} p(r|s)p(s)}{\sum_{s\in S_i^{(1)}} p(r|s)p(s)}\right) \\ &= \ln\left(\frac{\sum_{s\in S_i^{(0)}} \exp\left(-|r-s|^2/\sigma^2\right)}{\sum_{s\in S_i^{(1)}} \exp\left(-|r-s|^2/\sigma^2\right)}\right), \end{aligned} \tag{8}$$

where σ^2 is the variance of Gaussian noise. Equation (8) is called log-MAP and can be used to obtain LLR.

We can conclude that many exponential calculations are required in (8), making it inefficient and time-consuming. Fortunately, the approximate relation can be employed:

$$\begin{aligned} \Lambda_i(r) &= \ln\left(\frac{\exp\left(-\left|r-\widehat{S}_i^{(0)}(r)\right|^2/\sigma^2\right)}{\exp\left(-\left|r-\widehat{S}_i^{(1)}(r)\right|^2/\sigma^2\right)}\right) \\ &= \frac{1}{\sigma^2}\left(\left|r-\widehat{S}_i^{(1)}(r)\right|^2 - \left|r-\widehat{S}_i^{(0)}(r)\right|^2\right), \end{aligned} \tag{9}$$

where $\widehat{S}_i^{(0)}(r)$ and $\widehat{S}_i^{(1)}(r)$ are the nearest bits to the received signal point r in set $S_i^{(0)}$ and $S_i^{(1)}$. Equation (9) is called max-log-MAP. Compared with log-MAP, max-log-MAP demands no exponential calculation; the computation process can be simplified and the calculation time reduced. Nevertheless, the calculation for the smallest value of $|r-s|$ still has considerable computational complexity.

3 | SIMPLIFIED DE-MAPPING METHOD

The traditional de-mapping techniques previously mentioned suffer from considerable calculations and some of them require a detailed look-up table to execute many decisions. In this section, we propose a de-mapping method that can simplify the process with a limited performance loss of bit error rate (BER). In the proposed method, we take full advantage of the symmetric characteristics of each symbol mapping and divide the complex plane into several regions to employ the same calculation formula, which can be simplified.

3.1 | Symmetry analysis

The mapping method of 64-APSK modulation is Gray mapping. Here, b_5, b_4, b_3, b_2, b_1, and b_0 are used to represent the six bits transformed from each symbol of 64-APSK in the order from MSB to LSB. The two bits, b_5 and b_4, determine the quadrant where the signal point locates. It can be concluded from Figure 2 that each bit has a symbol mapping having symmetric characteristics with respect to the real or imaginary axis. The distribution of 0- and 1-points in b_5 is symmetric with respect to the real axis I, and is antisymmetric with the imaginary axis Q in b_4. For other b_i (i = 0, 1, 2, 3), the distribution of 0- and 1-points is symmetric with respect to both the real axis I and

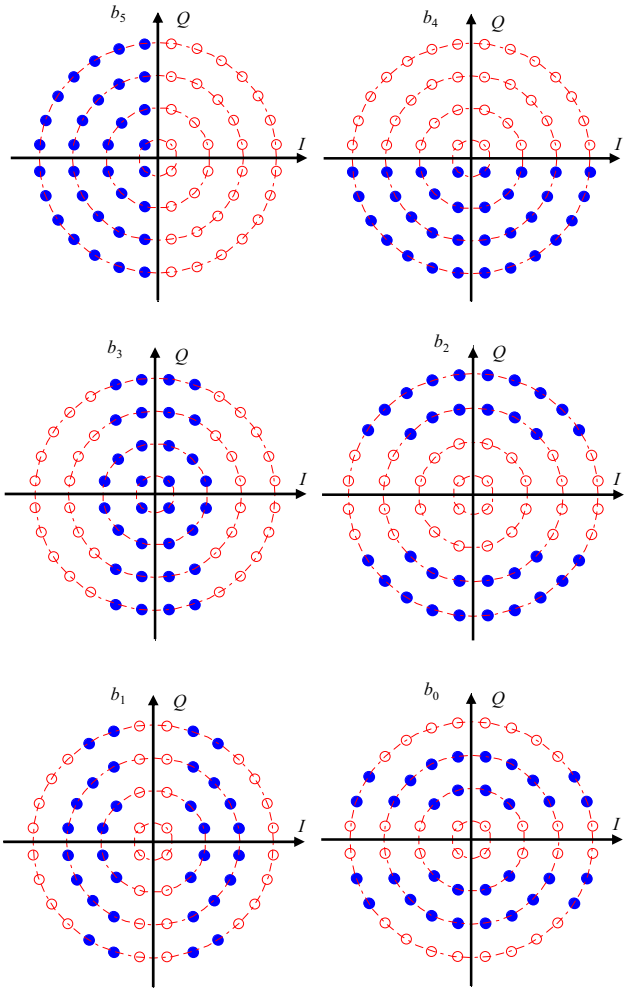

FIGURE 2 Symbol mapping of b_i

the imaginary axis Q. Consequently, the distributions of 0- and 1-points in any bit can be achieved from the first quadrant. In addition, the symbol mappings of b_5 and b_4, b_3 and b_2, and b_1 and b_0 are similar, which means that one symbol mapping can be obtained by rotating its counterpart. Specifically, the symmetric characteristics can be employed to simplify the calculation by mapping the received signal point to the first quadrant so that b_i can then be obtained.

3.2 | Formula simplification

All points of the 64-APSK constellation lie in different arcs and no point lies in the axes, which means that LLR is always calculated in the rectangular or polar coordinate system and that the values can hardly be determined. However, the calculations of LLR can be simplified by exploiting the positions in different coordinate systems.

Assume that two points $\widehat{S}_i^{(0)}(r)$ and $\widehat{S}_i^{(1)}(r)$, which lie in the same arc with radius R_i, are the nearest points to the received signal r with distance R_r. A is the intersection point of the line O_r and the arc with radius R_i. OB is the bisector of angle θ and θ' denotes the angle of AOB, as shown in Figure 3. According to (9), we can conclude that the distances $|r-\widehat{S}_i^{(1)}(r)|$ and $|r-\widehat{S}_i^{(0)}(r)|$ must be calculated before $\Lambda_i(r)$, which yields complicated calculation processes in both the rectangular and polar coordinate systems. To simplify the calculation, arc $\widehat{S}_i^{(0)}(r)A$ and arc $\widehat{S}_i^{(1)}(r)A$ are used to replace the distances $\widehat{S}_i^{(0)}(r)r$ and $\widehat{S}_i^{(1)}(r)r$:

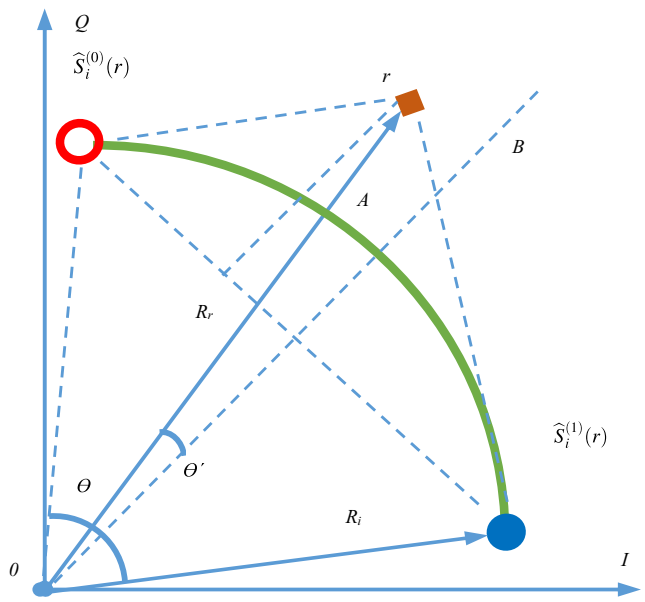

FIGURE 3 Simplified diagram to calculate the log likelihood ratio

$$\begin{aligned}\Lambda_i(r) &= \frac{1}{\sigma^2}\left(\left|r-\widehat{S}_i^{(1)}(r)\right|^2-\left|r-\widehat{S}_i^{(0)}(r)\right|^2\right)\\ &\approx \frac{1}{\sigma^2}\left(\left|\widehat{S}_i^{(1)}(r)A\right|^2-\left|\widehat{S}_i^{(0)}(r)A\right|^2\right)\\ &= \frac{1}{\sigma^2}\left(\left|R_i\times\left(\frac{\theta}{2}+\theta'\right)\right|^2-\left|R_i\times\left(\frac{\theta}{2}-\theta'\right)\right|^2\right)\\ &= \frac{2}{\sigma^2}R_i^2\theta\theta'.\end{aligned} \tag{10}$$

Similarly, when r lies on the same side as $\widehat{S}_i^{(1)}(r)$ of line OB, $\Lambda_i(r)$ is:

$$\begin{aligned}\Lambda_i(r) &= \frac{1}{\sigma^2}\left(\left|r-\widehat{S}_i^{(1)}(r)\right|^2-\left|r-\widehat{S}_i^{(0)}(r)\right|^2\right)\\ &\approx \frac{1}{\sigma^2}\left(\left|\widehat{S}_i^{(1)}(r)A\right|^2-\left|\widehat{S}_i^{(0)}(r)A\right|^2\right)\\ &= \frac{1}{\sigma^2}\left(\left|R_i\times\left(\frac{\theta}{2}-\theta'\right)\right|^2-\left|R_i\times\left(\frac{\theta}{2}+\theta'\right)\right|^2\right)\\ &= -\frac{2}{\sigma^2}R_i^2\theta\theta'.\end{aligned} \tag{11}$$

For a ring in the 64-APSK constellation, R_i and θ are constants, and thus, we must compute only θ':

$$\Lambda_i(r) = \frac{2R_i^2\theta}{\sigma^2}g(r)\theta'. \tag{12}$$

Here, $g(r)=\begin{cases}1, & r \text{ lies in } \widehat{S}_i^{(0)}(r) \text{ side of line } OB\\ -1, & r \text{ lies in } \widehat{S}_i^{(1)}(r) \text{ side of line } OB\end{cases}$.

3.3 | Complex plane partition

For a pair of $\widehat{S}_i^{(0)}(r)$ and $\widehat{S}_i^{(1)}(r)$ that lies in a horizontal or vertical line, the simplified calculation has been verified in [19]. When they lie in an arc or in a radius, the calculation has been simplified in (12).

To reduce the computational complexity, a rule known as "four lines" is set to simplify the LLR calculation of $\widehat{S}_i^{(0)}(r)$ and $\widehat{S}_i^{(1)}(r)$. The rule states whether they are approximately located in a horizontal or vertical line, in an arc, or in a radial line. Based on this rule, the symbol mapping can be divided into several partitions and the LLR of different pairs of $\widehat{S}_i^{(0)}(r)$ and $\widehat{S}_i^{(1)}(r)$ in the same partition can be calculated with the same simplified formula.

Because the symbol mapping of each b_i is symmetric with respect to the real or imaginary axis, only the symbol mapping in the first quadrant is illustrated in Figure 4.

A partition is unnecessary for the symbol mapping of b_4 and b_5, as only one type of point exists in its first quadrant. In the symbol mapping of b_2, all 1-points lie in the third quadrant and outermost ring, and the entire region is separated into two parts by a selected radius. Specifically, the

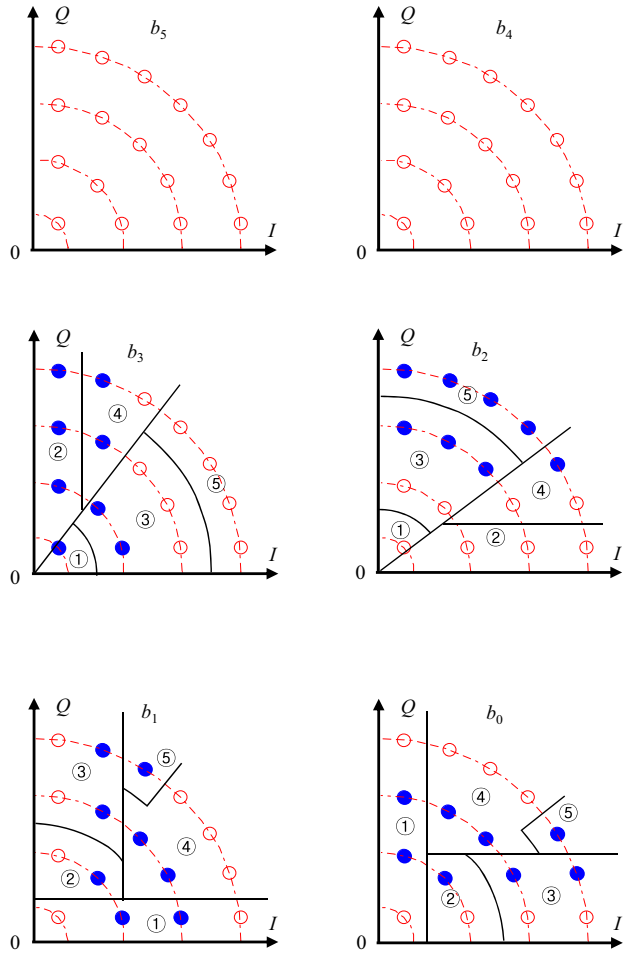

FIGURE 4 Divided complex plane of every b_i

polar angle of the selected radius is equal to the average of the polar angles of four points that locate in the two outermost rings and on the two sides of the radius. Partition ① is separated from other areas with an arc whose radius is $(R_2 + R_1)/2$. Only one 0-point exists in the partition, whereas the nearest 1-point lies in the third ring and is far from the center point. This allows us to conclude that they are in the same radial line. Partition ③ is an arc area with a radius bigger than $(R_2 + R_1)/2$ and smaller than $(R_4 + R_3)/2$. The 0- and 1-points in the second and third rings, respectively, are far from the center point, which means that the polar angles of $\widehat{S}_i^{(0)}(r)$ and $\widehat{S}_i^{(1)}(r)$ are similar and in the same radius. Partition ⑤ is composed of 1-points, whereas the nearest 0-points lie in the second ring, which indicates that the polar angles of $\widehat{S}_i^{(0)}(r)$ and $\widehat{S}_i^{(1)}(r)$ are similar and in the same radius. In partition ②, three 0-points exist that have a similar y coordinate, and the nearest 1-points with a similar y coordinate are in the third and the outermost rings. Here, we consider that the 0-points and the nearest 1-points lie in the same vertical line. In partition ④, every two 0-points and their corresponding nearest 1-points are in the same arc. Partition ② and ④ are divided by a line that is parallel to the real axis and the line's ordinate is equal to the average ordinates of five 1-points on both sides of the line.

The symbol mapping of b_3 is antisymmetric to that of b_2 with respect to the 45° line and the partition is symmetric to the mapping of b_2 with respect to the 45° line. The symbol mapping of b_0 is separated into five partitions. Partition ① is divided by a line that is parallel to the imaginary axis and has an abscissa equal to the average abscissa of eight points on both sides. As the abscissae of 0- and 1-points are similar, they can be approximately regarded as being on the same vertical line. Similarly, partitions ④ and ⑤ are divided from partitions ② and ③ by a line that is parallel to the real axis and has an ordinate equal to the average ordinate of five 1-points on both sides. In addition, the partitions ② and ③ is divided by an arc with a radius equal to the average value of R_1 and R_2. In partition ②, it is clear that 0- and 1-points are located on the same arc. For partition ③, the pairs of 0- and 1-points on the same arc are in the vertical lines. Furthermore, partition ⑤ is separated from partition ④ by an arc in the middle of the outermost and inner rings. In addition, a perpendicular bisector between the point in partition ⑤ and its adjacent point in the outermost ring can be obtained. Regarding partition ④, the 0- and 1-points in the outermost and third rings, respectively, are far from the center point, which means that the polar angles of $\widehat{S}_i^{(0)}(r)$ and $\widehat{S}_i^{(1)}(r)$ are similar, and they are in the same radius. Therefore, only one 1-point is present in partition ⑤, and the nearest 0-point to its neighbor lies in the outermost ring.

The symbol mapping of b_1 and the corresponding partition are both symmetric to b_0 with respect to the 45° line. Computational formulas of LLRs in the partitions of each b_i are listed in Table 1 (at the end of this article). In this study, the common factor $2/\sigma^2$ is abridged, and y_1 and y_0 are the ordinate values of 1- and 0-points, respectively. In addition, R_i $(i = 1, 2, 3, 4)$ denotes the radius of the ring.

In the partition, we use approximation to decrease the computational complexity and partition numbers. Theoretically, a more precise result involves a smaller partition size. However, this leads to a greater number of calculations.

4 | CALCULATION ANALYSIS

For the proposed method, different positions of the received signal in the 64-APSK constellation lead to different numbers of calculations. In this section, we assume that the locations of the received signals are uniformly distributed in the global constellation, and we neglect the calculation for ρ and θ.

TABLE 1 Formulas for calculating log likelihood ratio

	b_0	b_2	b_4
①	$(y_1 - y_0)\left(\frac{y_1+y_0}{2} - Q_r\right)$	$(R_3 - R_1)\left(\frac{R_3+R_1}{2} - \rho_r\right)$	Q_r
②	$R_2^2 \times \frac{\pi}{6} \times \left(\frac{\pi}{6} - \theta_r\right)$	$(y_1 - y_0)\left(\frac{y_1+y_0}{2} - Q_r\right)$	
③	$(y_1 - y_0)\left(\frac{y_1+y_0}{2} - Q_r\right)$	$(R_3 - R_2)\left(\frac{R_3+R_2}{2} - \rho_r\right)$	
④	$(R_3 - R_4)\left(\frac{R_3+R_4}{2} - \rho_r\right)$	$(y_1 - y_0)\left(\frac{y_1+y_0}{2} - Q_r\right)$	
⑤	$-R_4^2 \times \frac{\pi}{14} \times \left(\frac{3\pi}{14} - \theta_r\right)$	$(R_4 - R_2)\left(\frac{R_4+R_2}{2} - \rho_r\right)$	

TABLE 2 Computational complexity comparisons for de-mapping methods

	Log-MAP	Max-Log-MAP	Simplified method
Multiplication	192	128	2
Addition and subtraction	564	198	2
Exponent and logarithm	70	0	0
Judgment	0	372	5.6

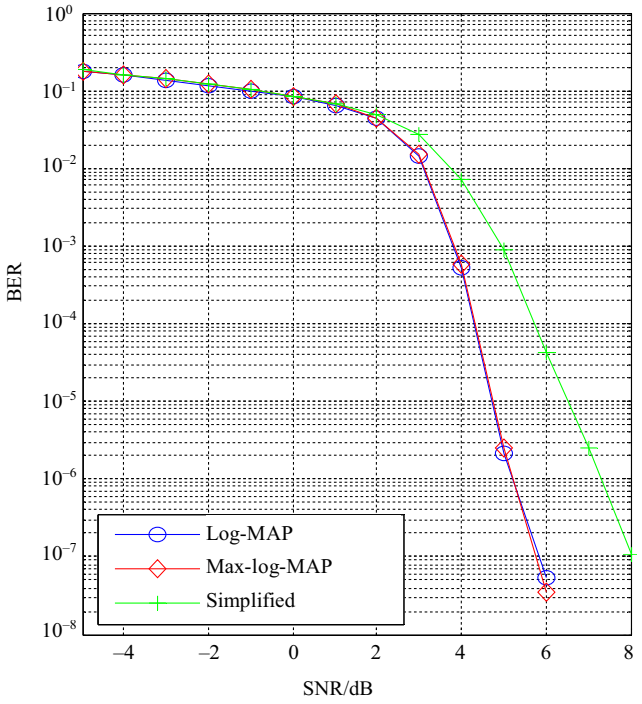

FIGURE 5 Performance comparison of de-mapping methods over the AWGN channel

The computational complexity of the methods previously mentioned is shown in Table 2. This clearly reveals that, in the process of de-mapping a received signal of 64-APSK with the log-MAP method, more than 564 times the number of additions and subtractions, 192 times the number of multiplications, and approximately 70 times the number of exponents and logarithms are required. The computational complexity of max-log-MAP clearly does not diminish for any of the exponents and logarithms used, whereas 198 times the number of additions and subtractions, 128 times the number of multiplications, and 372 times the number of judgments are still required. However, the proposed simplified de-mapping method demands only twice the number of addition and subtraction operations, which are roughly reduced to 1/96 and 1/64, respectively, compared with log-MAP and max-log-MAP. The multiplication operations are also reduced to twice the number of times, to only 1/282 and 1/99, respectively, compared with log-MAP and max-log-MAP. In addition to these, only approximately 5.6 times the number of judgments are required. That the computational complexity is significantly reduced is obvious.

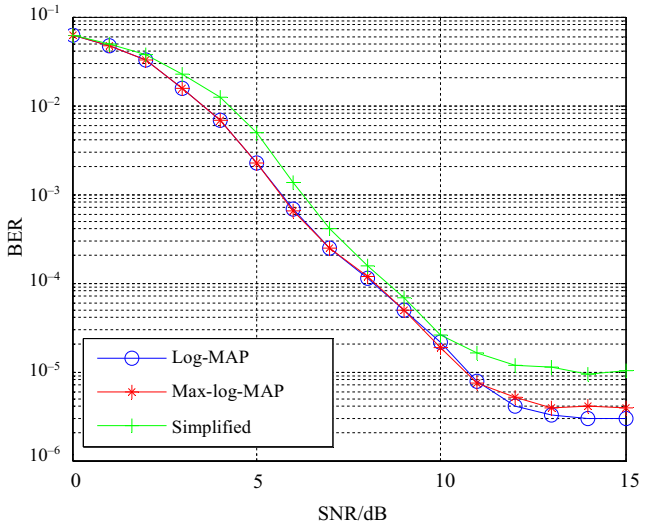

FIGURE 6 Performance comparison of de-mapping methods over the Rayleigh fading channel

TABLE 3 Time consumption comparison of de-mapping methods

De-mapping method	Time/s
Log-MAP	75,156
Max-log-MAP	41,358
Simplified method	5,981

5 | SIMULATION RESULTS

The BER performance of the proposed method was evaluated through simulation. Here, the ratio of the 64-APSK constellation was selected to be R_1:R_2:R_3:R_4 = 1:2.73:4.52:6.31, according to [2]. The SNR over AWGN channel was varied from −5 dB to 8 dB with a step size of 1 dB, and from 0 dB to 15 dB for the Rayleigh fading channel with a step size of 1 dB. The simulation was run 1,000,000

times, and 1,600 random signal bits were transmitted each time. We utilized LDPC codes and the belief propagation (BP) decoder over both channels. For the sake of comparison, we plot the BER performance of the three kinds of de-mapping methods against the SNR together in Figures 5 and 6, and their time consumptions are listed in Table 3.

Figure 5 shows the BER performance plotted over the AWGN channel. As the figure shows, the three methods had similar BER performance trends. In other words, they tended to decrease with each increase in SNR. In addition, the BER performance of the simplified method was slightly lower than that of log-MAP and max-log-MAP. For the latter two methods, the BER value decreased to zero when SNR was 6 dB, whereas it was 8 dB for the simplified method.

The performance plot of the three methods over the Rayleigh fading channel is shown in Figure 6. The figure shows that the plot of the simplified method was nearly coincident with that of log-MAP and max-log-MAP, meaning the performance of the simplified method was similar to that of the latter two. In addition, we can also see that an error floor appears when SNR is more than 11 dB. This is because the example used here is LDPC. In practice, code that is more suitable should be used to diminish or avoid the effect of an error floor.

Figures 5 and 6 show that the BER performance of the simplified method was not as good as that of log-MAP and max-log-MAP. This was because simplification and approximation were used to reduce the computational complexity during the process of calculating LLR with the simplified method.

The different time consumptions of the three methods of de-mapping are presented in Table 3; here, the decoding time was not considered. The table shows that time consumption of the simplified method was far less than that of log-MAP and max-log-MAP. When compared to the max-log-MAP, the time consumption of the simplified method was approximately 14.5%, whereas it was only 8.0% when compared with log-MAP.

The decrease in time consumption of the simplified method was due to the reduction in the number of calculations of multiplication, addition, subtraction, and judgment as compared with max-log-MAP. In addition, the simplified method even reduced the number of exponent and logarithm calculations when compared with log-MAP.

6 | CONCLUSION

In this study, we proposed a low-complexity de-mapping method by taking full advantage of the symmetric characteristics of a 64-APSK constellation. In this method, only the 0- and 1-points in the first quadrant were investigated based on the symmetric characteristics of the symbol mapping. The points in the first quadrant were then separated into different partitions to simplify the calculation formulas. In addition, LLR could be achieved immediately with the positions of the received signals. Simulations were conducted to verify that the proposed simplified de-mapping method had limited performance degradation when 64-APSK signals were transmitted over the AWGN and Rayleigh fading channels, whereas the time consumption was considerably reduced to approximately 14.5% or even as low as approximately 8.0% as compared with max-log-MAP and log-MAP, respectively. In other words, the proposed low-complexity method decreased BER performance slightly with a drastic decrease in time consumption.

ORCID


Junwei Bao https://orcid.org/0000-0002-9428-3886

REFERENCES

1. R. D. Gaudenzi et al., *Performance analysis of Turbo-coded APSK modulations over nonlinear satellite channels*, IEEE Trans. Wirel. Commun. **5** (2006), no. 9, 2396–2407.
2. CCSDS 131.2-B-1, *Recommendation for space data system standards: Flexible advanced coding and modulation scheme for high rate telemetry applications*, The Consultative Committee for Space Data Systems (CCSDS), Washington, DC, USA, 2012.
3. ETSI EN 302 307 v1.2.1, *Digital video broadcasting (DVB); Second generation framing structure, channel coding and modulation systems for broadcasting, interactive services, news gathering and other broadband satellite applications (DVB-S2)*, European Telecommunications Standards Institute, France, 2009.
4. E. Yao et al., *A simplified soft decision demapping algorithm of 16-APSK signals in AWGN channel*, in Int. Conf. Netw. Security, Wireless Commun. Trusted Comput., Wuhan, China, Apr. 2010, pp. 103–106.
5. K. Cho et al., *An approximated soft decoding algorithm of 16-APSK signal for DVB-S2*, in Int. Conf. Consumer Electron., Hiroshima, Japan, Jan. 2007, pp. 1–2.
6. J. Lee et al., *Soft-decision demapping algorithm with low computational complexity for coded 4+12 APSK*, Int. J. Satell. Commun. Netw. **31** (2013), no. 3, 103–109.
7. M. Zhang et al., *Efficient soft demodulation scheme for digital video broadcasting via satellite – second generation system*, IET Commun. **8** (2014), no. 1, 124–132.
8. M. Anedda et al., *64-APSK constellation and mapping optimization for satellite broadcasting using genetic algorithms*, IEEE Trans. Broadcast. **62** (2016), no. 1, 1–9.
9. X. Xiang et al., *Constellation labeling optimization for bit-interleaved coded APSK*, Sensors Syst. Space Appl. IX **98380Q**, (2016), 1–11.
10. A. R. Ndjiongue et al., *Closed-form SER expression for APSK based on the kite structure*, IEEE Commun. Lett. **21** (2017), no. 10, 2181–2185.

11. M. Sandell et al., *Efficient demodulation of general APSK constellations*, IEEE Signal Process. Lett. **23** (2016), no. 6, 868–872.
12. Q. Xie et al., *Simplified soft demapper for APSK with product constellation labeling*, IEEE Trans. Wirel. Commun. **11** (2012), no. 7, 2649–2657.
13. M. Zhang et al., *Near ML soft bit estimation for APSK with very low complexity*, in Vehicular Technol. Conf., Nanjing, China, May 2016, pp. 1–5.
14. K. Yan et al., *Non-uniform APSK optimization for BICM systems*, Tsinghua Sci. Technol. **20** (2015), no. 2, 175–181.
15. S. H. Choi et al., *The mapping and demmaping algorithms for high order modulation of DVB-S2 systems*, in Asia-Pacific Conf. Commun., Busan, Rep. of Korea, Aug. 2006, pp. 1–5.
16. V. B. Olivatto et al., *Simplified method for log-likelihood ratio approximation in high-order modulations based on the Voronoi decomposition*, IEEE Trans. Broadcast. **63** (2017), no. 3, 1–7.
17. W. You et al., *An efficient soft de-mapping algorithm for APSK signals*, in Int. Conf. Mechatronics Inform. Technol., Shenzhen, China, Aug. 2016, pp. 100–104.
18. E. Larsson et al., *Fixed-complexity soft MIMO detection via partial marginalization*, IEEE Trans. Signal Process. **56** (2008), no. 8, 3397–3407.
19. L. Wang et al., *A simplified bit metric calculation method for high-order PSK*, Sci. China **56** (2012), no. 7, 1–9.

AUTHOR BIOGRAPHIES

Junwei Bao received his BS degree in physics education from Dalian University, Dalian, China, in 2001, and his MS degree in condensed matter physics from Sichuan University, Chengdu, China, in 2005. Since 2005, he has been with the College of Science, Nanjing University of Aeronautics and Astronautics (NUAA), Nanjing, China, where he is now a lecturer. He is now working toward his PhD degree in the College of Electronic and Information Engineering, NUAA, Nanjing, China. His research is focused on signal processing and wireless communications.

Dazhuan Xu received his BS degree from Nanjing Institute of Technology, Nanjing, China, in 1983. He received his MS and PhD degrees in communication and information systems from Nanjing University of Aeronautics and Astronautics (NUAA) in 1986 and 2001, respectively. He has been with the College of Electronic and Information Engineering, NUAA, Nanjing, China, where he is a full professor. His research interests include digital communications, software radio, and coding theory.

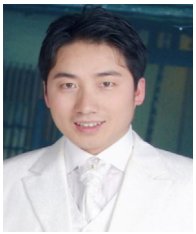

Xiaofei Zhang received his MS degree in electrical engineering from Wuhan University, Wuhan, China, in 2001, and his PhD degree in communication and information systems from Nanjing University of Aeronautics and Astronautics (NUAA), China, in 2005. He has been with the College of Electronic and Information Engineering, NUAA, Nanjing, China, where he is a professor His research is focused on array signal processing and communication signal processing.

Hao Luo received his ME degree in communication and information systems from Nanchang Hangkong University, Nanchang, China, in 2011. Currently, he is working toward his PhD degree in communication and information systems at Nanjing University of Aeronautics and Astronautics, Nanjing, China. His research interests are in the broad areas of signal processing, wireless communications, and information theory.